Journal of
Synchrotron
Radiation

ISSN 0909-0495

Received 28 May 2008
Accepted 17 August 2008

Influence of crystallographic orientation of biogenic calcite on *in situ* Mg XANES analyses

Alberto Pérez-Huerta,[a]* Maggie Cusack,[a] Markus Janousch[b] and Adrian A. Finch[c]

[a]Department of Geographical and Earth Sciences, University of Glasgow, UK, [b]Swiss Light Source, Paul Scherrer Institute, Switzerland, and [c]School of Geography and Geosciences, University of St Andrews, UK. E-mail: alberto.perezhuerta@ges.gla.ac.uk

Micro X-ray absorption near-edge spectroscopy at the Mg *K*-edge is a useful technique for acquiring information about the environment of Mg^{2+} in biogenic calcite. These analyses can be applied to shell powders or intact shell structures. The advantage of the latter is that the XANES analyses can be applied to specific areas, at high (*e.g.* micrometre) spatial resolution, to determine the environment of Mg^{2+} in a biomineral context. Such *in situ* synchrotron analysis has to take into account the potential effect of crystallographic orientation given the anisotropy of calcite crystals and the polarized nature of X-rays. Brachiopod shells of species with different crystallographic orientations are used to assess this crystallographic effect on *in situ* synchrotron measurements at the Mg *K*-edge. Results show that, owing to the anisotropy of calcite, *in situ* X-ray absorption spectra (XAS) are influenced by the crystallographic orientation of calcite crystals with a subsequent potentially erroneous interpretation of Mg^{2+} data. Thus, this study demonstrates the importance of crystallography for XAS analyses and, therefore, the necessity to obtain crystallographic information at high spatial resolution prior to spectroscopic analysis.

Keywords: brachiopods; calcite; XAS; crystal lattice; *c*-axis.

1. Introduction

Mg/Ca ratios of biogenic calcite of marine invertebrate organisms, such as foraminifera and mollusc shells, have been successfully used to determine seawater temperature, without the influence of salinity such as in the oxygen isotope measurements (*e.g.* Elderfield & Ganssen, 2000). Mg/Ca thermometry is based on the principle that there is an increase in Mg^{2+} substituting for Ca^{2+} within the crystal lattice with an increase in temperature (Elderfield & Ganssen, 2000; Lear *et al.*, 2000). This dependence is observed in studies using abiogenic calcite. Biominerals are composites of organic and mineral phases and, while a significant fraction of magnesium may be present in the lattice, some magnesium may be in a different environment such as in association with specific organic components (*e.g.* protein). X-ray absorption near-edge spectroscopy (XANES) analysis at the Mg *K*-edge makes it possible to determine the local environment of Mg^{2+} within biogenic calcite. The possibility of performing such micro-XANES (μ-XANES) analyses *in situ* is attractive since it provides fine spatial resolution that assists our understanding of biomineralization and improves our interpretation of climate proxies (*e.g.* Pingitore *et al.*, 1992; Parkman *et al.*, 1998). The use of this synchrotron technique for *in situ* analyses, however, would have to take into account the effect of crystallographic orientation of calcite crystals since calcite is anisotropic (space group *Rc*) and X-rays from the symmetry plane of a synchrotron are linearly polarized. Therefore, the absorption (the dipole absorption cross section) depends on the polarization and light beam direction with respect to the crystal axes (Brouder, 1990). The micro-crystallites in shells are not randomly oriented but usually show variable degrees of crystal alignment which are strongly dependent on shell architecture. This problem becomes more acute as progressively smaller beams are used. For example, anisotropy in the Sr *K* X-ray absorption spectra of coral aragonite was observed by Allison *et al.* (2005).

Here, we analyse the effects of crystallography on the determination of Mg^{2+} in biogenic calcites by μ-XANES at the Mg *K*-edge using brachiopod shells. A species of rhynchonelliform brachiopod, *Terebratulina retusa*, with low-Mg calcite, and a craniid brachiopod, *Novocrania anomala*, with high-Mg calcite, are used in this study [for further information on the biology of these species see Pérez-Huerta *et al.* (2007) and Pérez-Huerta & Cusack (2008)] (Fig. 1). Besides the dissimilar magnesium content, both species have a different overall crystallographic orientation of calcite crystals (Fig. 2). XAS measurements were carried out in anterior shell regions of dorsal valves, the most recent area of the shell growth, where there is crystallographic uniformity in both species across the majority of shell thickness ('secondary layer') (Pérez-Huerta & Cusack, 2008). Although there is a uniform

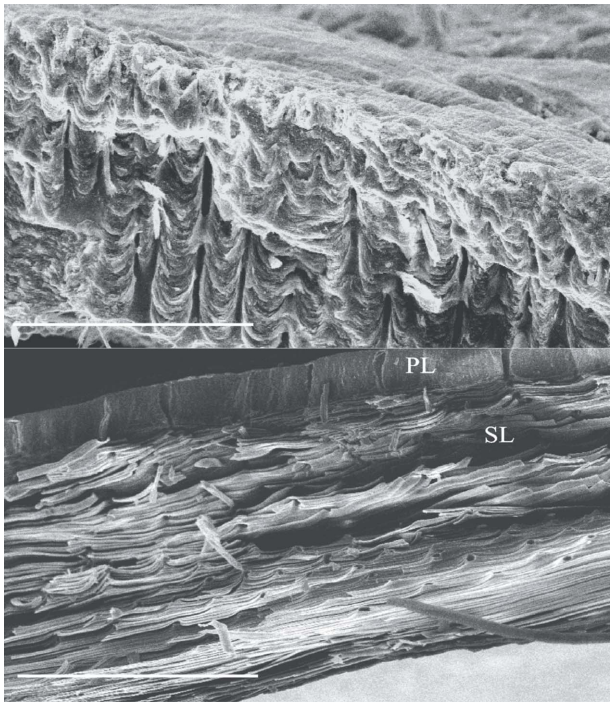

Figure 1
Scanning electron micrographs of the shell microstructure in *Novocrania anomala* (top), showing the undulating laminae in the secondary layer, and *Terebratulina retusa* (bottom), showing the primary layer (PL) and secondary layer (SL) comprising calcite fibres. Scale bar = 200 µm. Images courtesy of J. England.

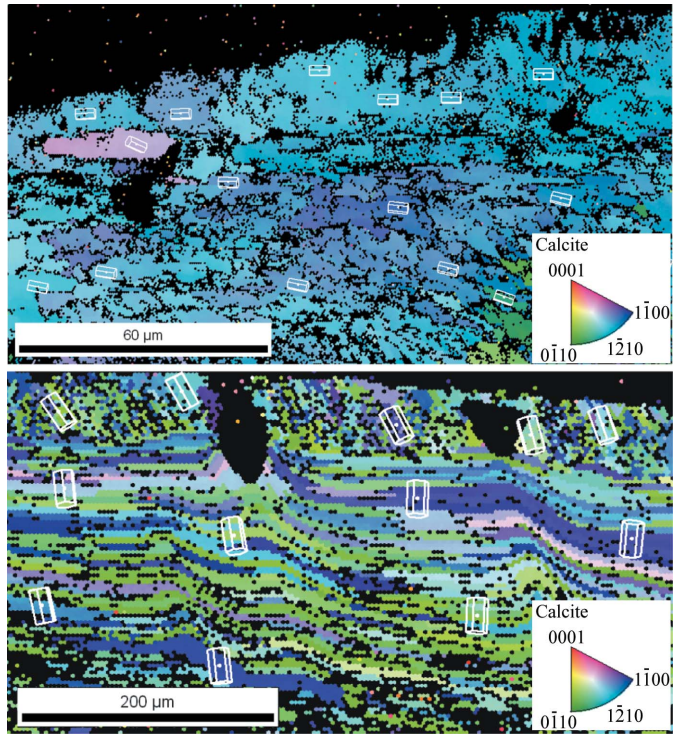

Figure 2
Crystallographic orientation maps, with colour key indicating which crystallographic plane is normal to the plane of view, obtained by electron backscatter diffraction showing the orientation of calcite crystals, indicated by wire frames, in the anterior regions of dorsal valves of *Novocrania anomala* (top) and *Terebratulina retusa* (bottom). The uniformity of colour on 10 µm scales demonstrates that the sample is crystallographically non-random at the scales of the X-ray spot.

crystallographic orientation within each species, that orientation differs between the two species. In *N. anomala* the *c*-axis of calcite crystals is oriented parallel to the outer-shell surface while the *c*-axis orientation is perpendicular in *T. retusa* (Fig. 2).

2. Methodology

2.1. Sample preparation

Living specimens of *Terebratulina retusa* and *Novocrania anomala* were collected from the Firth of Lorn, Oban, NW Scotland (56° 24′ N, 5° 38′ W). Samples were obtained from a depth of 200 m by dredging. Specimens were stored in seawater and transported to the University of Glasgow. Valves were disarticulated and the pedicle and soft tissues removed using dental tools. Valves were cleaned in an ultrasonic bath using an aqueous solution of sodium hypochlorite (1% *v*/*v*) and thoroughly rinsed in MilliQ water. Fragments of anterior regions of dorsal valves were embedded in epoxy resin in 1 cm-diameter cylindrical blocks of 0.5 cm thickness and the shell sections polished through a series of grinding and polishing discs. Initially the sample surface was ground down using diamond-impregnated papers at 74 µm and then 20 µm; diamond slurry at 8 µm then 6 µm are followed by a compound diamond pad at 6 µm then 3 µm. The polishing stages were performed with alpha aluminium oxide at 1 µm and 0.3 µm with a final polish with 0.06 µm colloidal silica on a short nap disc. Shell fragments were also crushed and ground to obtain powder samples for comparison.

2.2. Electron backscatter diffraction (EBSD)

EBSD data were obtained using a *QUANTA* FEI 200F field-emission scanning electron microscope (SEM) equipped with a TSL EBSD system running *OIM* version 5. The SEM was operated in high-vacuum mode at 20 kV with spot size of 4 and aperture size of 4. Final EBSD data sets were partitioned to remove all grains that had a confidence index of less than 0.1 using *OIM* software from EDAX.

2.3. XANES analyses

XANES analyses were carried out at the Lucia beamline of the Swiss Light Source at the Paul Scherrer Institute, Switzerland (Flank *et al.*, 2006). This beamline uses an APPLE-II-type undulator as its source of X-rays. It allows the linear polarization to be changed from horizontal (0°) to vertical (90°) without the need to rotate the sample. µ-XANES data were collected by scanning X-rays between 1300 and 1364 eV in a beam of width 4.5 µm and height 10 µm, recording the fluorescence yield of the Mg *Kα* secondary radiation using a silicon drift diode detector. The active area of the detector is 10 mm^2 and has an energy resolution of about 120 eV at the Mg *K*-edge at a maximum count rate of about 10^5 s^{-1}. The

samples were glued onto a copper plate, which was mounted perpendicular to the incoming beam. The fluorescence detector made an angle of 12° with respect to the sample surface. This grazing-exit set-up allows the so-called 'self-absorption effect' for concentrated samples to be minimized (Grolimund *et al.*, 2004). Resulting spectra were obtained throughout averaging four to six scans in each analysis with about 8 h of acquisition time per four scans. Data were processed using *Athena* software version 0.5.084 (http://cars9.uchicago.edu/~ifeffit/).

3. Results

X-ray absorption spectra (XAS) were obtained for measurements *in situ* of shell sections and powders of both species (Fig. 3). The XAS of *T. retusa* and *N. anomala* are quite different for analyses of single points on calcite shell. In *T. retusa* there is a peak near 1310 eV and a double peak at 1320 eV, both of which being absent in the spectrum of *N. anomala* (Fig. 3, top). In addition, *N. anomala* shows a higher intensity in the white line and broader main peak beyond 1310 eV (Fig. 3, top). Based on these spectra, one may conclude that the observations are due to differences in the location of Mg^{2+} between the two species or to different crystal orientation effects. Results from powder samples of both species, however, show the same overall spectra (Fig. 3, bottom), demonstrating that the Mg^{2+}, on average, is in the same environment in the two different shells.

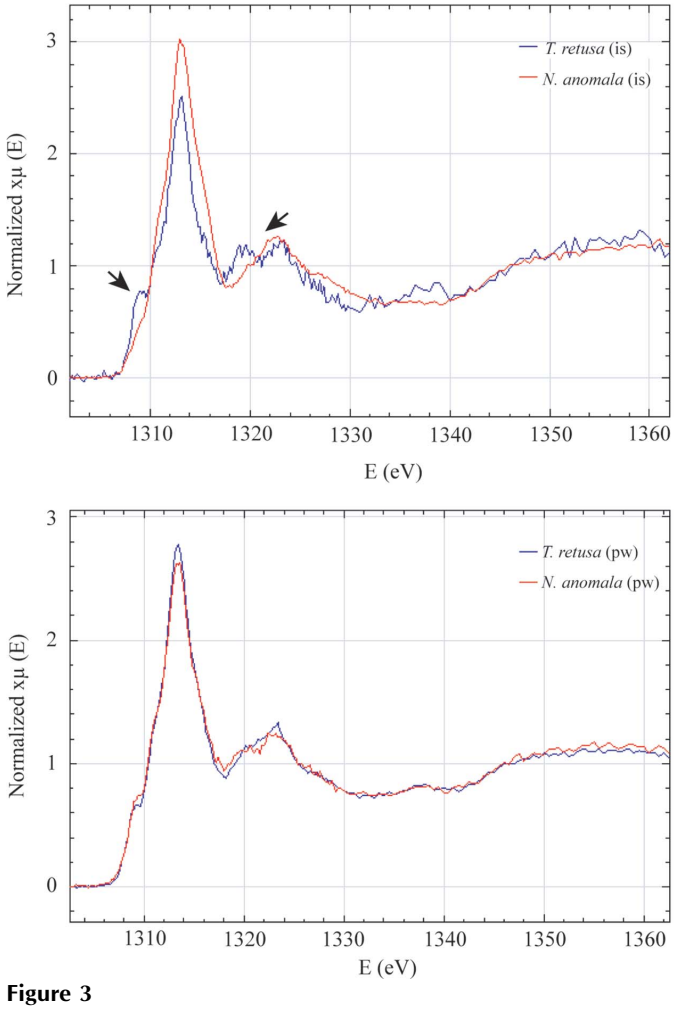

Figure 3
X-ray absorption spectra from *in situ* analyses of shell structures (is) [top; arrows indicate regions in the spectra with major differences] and powders (pw) [bottom] in *Novocrania anomala* and *Terebratulina retusa*.

4. Discussion

Comparison of X-ray absorption spectra from measurements *in situ* and powders indicates that differences relate to the crystallographic orientation of calcite biominerals (Fig. 2). One way to test this hypothesis is to obtain spectra under different sample orientations and/or polarizations of the X-ray light and thus reveal the angular dependence of the X-ray absorption coefficient.

In the dipole approximation and for a dichroic (also known as 'uniaxial') sample (*i.e.* materials of tetragonal, trigonal and hexagonal symmetry; Brouder, 1990) the absorption coefficient $\mu(\theta)$ depends on the angle θ between the polarization direction and the crystal's principal axis (here the *c*-axis),

$$\mu(\theta) = \mu_{\parallel} \sin^2\theta + \mu_{\perp} \cos^2\theta. \quad (1)$$

Here, $\mu_{\parallel}$ and $\mu_{\perp}$ are the absorption coefficients for the polarization vector being parallel ($\theta = 0°$) or perpendicular ($\theta = 90°$), respectively, to the main crystal axis. A consequence of this angular dependence is that the averaged absorption coefficient μ, *i.e.* measured on a textureless powder, is given by

$$\mu = (\mu_{\parallel} + 2\mu_{\perp})/3. \quad (2)$$

These equations are applicable to trigonal calcite as in the present study, although more complex equations are valid for lower symmetry minerals such as aragonite. In the case of *N. anomala*, the crystallographic orientation of the granules is parallel to the shell surface and perpendicular for *T. retusa*. Owing to the angular dependence of the absorption coefficient, one has to compare spectra of both shells taken with the same angle θ between the *c*-axis of the crystallites and the polarization direction. This is the case in Fig. 4, where $\theta = 90°$ for both shells and, indeed, the two spectra are essentially the same.

For an additional test of our hypothesis we apply equation (2). In Fig. 5 we show the absorption for $\theta = 90°$ and $\theta = 0°$ as well as the sum according to (2) of the two spectra, together with the measured powder spectrum. The overall agreement is quite good. Differences in the comparison of spectra in Fig. 4 are mainly due to the poor signal-to-noise ratio of some of the spectra and the scatter of the crystallite's orientations (*cf.* Fig. 2).

XANES at the Mg *K*-edge is a useful technique for acquiring information about the Mg^{2+} location in biogenic calcite within biomineral structures. Our study, however, demonstrates the importance of crystallography and the profound effect of calcite anisotropy on XAS. In particular, this information is relevant since the angular dependence of

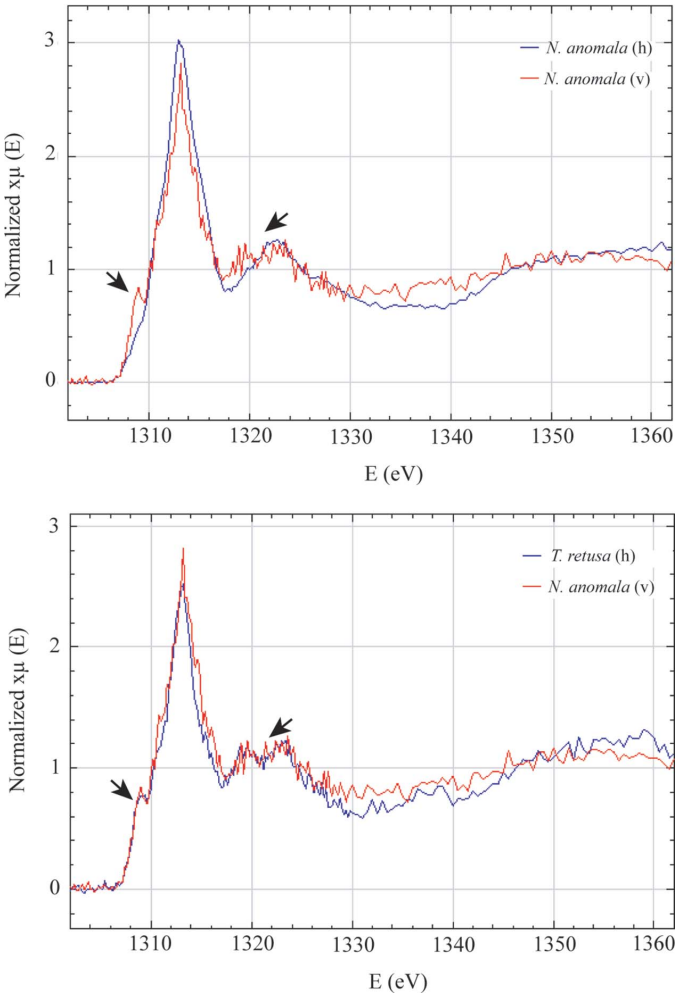

Figure 4
X-ray absorption spectra from *in situ* analyses in *Novocrania anomala* comparing the spectra with vertical (v) and horizontal (h) X-ray beam polarization [top] and the comparison of results with *Terebratulina retusa* [bottom] (arrows indicate areas for comparison within spectra).

the X-ray absorption coefficient (μ) is influenced by the crystallographic orientation of calcite crystals. Thus, the combination of crystallographic information and spectroscopy analysis will result in a powerful method to determine the atomic location of trace elements in calcium carbonate biominerals.

APH and MC acknowledge financial support from the BBSRC (BB/E003265/1). This research project has been supported by the European Commission under the 6th Framework Programme through the Key Action: Strengthening the European Research Area, Research Infrastructures (contract no: RII3-CT-2004-506008). J. Gilleece and P. Chung are also thanked for providing technical support. This work is a contribution to the BioCalc Project of the EuroMinScI Programme (ESF-EUROCORES, ERAS-CT-2003-980409) and the Theme 3 (Atmosphere, Oceans and Climate) of SAGES (Scottish Alliance for Geoscience, Environment and Society).

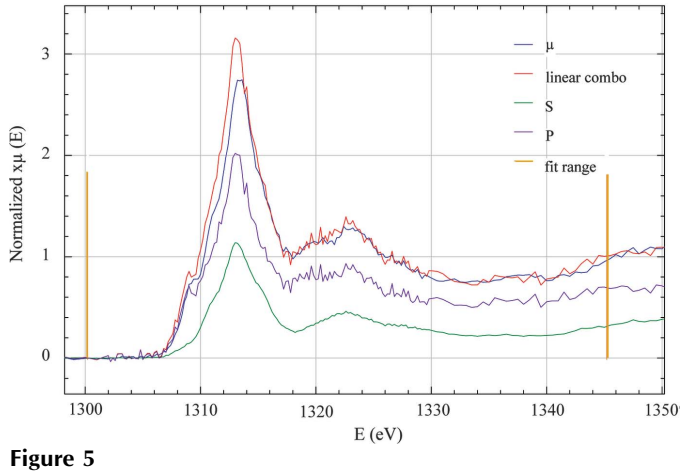

Figure 5
X-ray absorption spectra from *in situ* analyses in *Novocrania anomala* comparing the spectra of the absorption for $\theta = 90^\circ$ (P) and $\theta = 0^\circ$ (S) as well as the sum according to equation (2) in the text (linear combination) with respect to that of the powder (μ).

References

Allison, N., Finch, A. A., Newville, M. & Sutton, S. V. (2005). *Geochim. Cosmochim. Acta*, **69**, 3801–3811.
Brouder, Ch. (1990). *J. Phys. Condens. Matter*, **2**, 701–738.
Elderfield, H. & Ganssen, G. (2000). *Nature (London)*, **405**, 442–445.
Flank, A. M. *et al.* (2006). *Nucl. Instrum. Methods Phys. Res. B*, **246**, 269–274.
Grolimund, D. *et al.* (2004). *Spectrochim. Acta B*, **59**, 1627–1635.
Lear, C. H., Elderfield, H. & Wilson, P. A. (2000). *Science*, **287**, 269–272.
Parkman, R. H., Charnock, J. M., Livens, F. R. & Vaughan, D. J. (1998). *Geochim. Cosmochim. Acta*, **62**, 1481–1492.
Pingitore, N. E., Lytle, F. W., Davies, B. M., Eastman, M. P., Eller, P. G. & Larson, E. M. (1992). *Geochim. Cosmochim. Acta*, **56**, 1531–1538.
Pérez-Huerta, A. & Cusack, M. (2008). *Zoology*, **111**, 9–15.
Pérez-Huerta, A., Cusack, M., Zhu, W., England, J. & Hughes, J. (2007). *J. R. Soc. Interface*, **4**, 33–39.